Sigma Journal of Engineering and Natural Sciences
Web page info: https://sigma.yildiz.edu.tr
DOI: 10.14744/sigma.2024.00104

Research Article

The effect of LRB stiffness changes with and without supplemental viscous dampers on seismic responses of an experimentally verified mdof building

Adnan KIRAL[1], Zeliha TONYALI[1,*]

[1]*Department of Civil Engineering, Recep Tayyip Erdogan University, Rize, 53100, Türkiye*

ARTICLE INFO

Article history
Received: 21 February 2024
Revised: 26 June 2024
Accepted: 01 July 2024

Keywords:
Base Isolation System; Earthquake; Energy Dissipation Systems; Lead Rubber Bearings; Linear Time-History Analysis; Seismic Performance of a MDOF Building; Viscous Dampers

ABSTRACT

The structures are exposed to a significant amount of seismic energy released during large earthquakes. A base isolation system (BIS) is one of the most efficient solutions to mitigate seismic responses. However, only the BIS may not be sufficient as they can undergo increasing displacement demand in earthquake-prone zones due to the base isolators' inherent nonlinear behaviour. Supplemental viscous dampers and base isolation (BI) are one of the most effective ways to manage seismic responses while protecting the main structural system from permanent damage. The purpose of this study is to examine the effect of laminated rubber bearings (LRBs) stiffness change in the seismic reactions of an existing multi-story building with and without supplemental viscous dampers (VDs). To assess the effect of LRBs' stiffness on the seismic performance of the building, three different stiffness ratios (i.e., the sum of the stiffnesses of the first-floor columns (k_1) to the sum of the stiffnesses of LRB (k_b) were chosen, and these ratios (k_1/k_b) were 20, 40, and 80. The Sosokan building, which is situated at Keio University in Yokohama, Japan, was selected as an example. The building model was developed in MATLAB and verified with experimental results. The effects of LRB stiffness were examined by employing linear time-history analysis, both with and without viscous dampers on the displacement of the isolation layer, inter-story drift, and acceleration of the building. In this study, it is found that the displacements and accelerations at isolation floor and above levels significantly reduce in the LRB base isolated system equipped with viscous dampers (BI&VDs) as compared to BI (no VDs) model. Also, it is concluded that a proper damping coefficient (C_d) is important for the reduction of both displacement and acceleration at the same time. The finding of this study shows the importance of an optimal damping coefficient section in the adopted building model.

Cite this article as: Kiral A, Tonyali Z. The effect of LRB stiffness changes with and without supplemental viscous dampers on seismic responses of an experimentally verified mdof building. Sigma J Eng Nat Sci 2025;43(1):301–315.

*Corresponding author.
*E-mail address: zeliha.tonyali@erdogan.edu.tr

This paper was recommended for publication in revised form by Editor-in-Chief Ahmet Selim Dalkilic

Published by Yıldız Technical University Press, İstanbul, Turkey

INTRODUCTION

Türkiye is an earthquake-prone country, and there have been multiple moderate-to-large earthquakes in the last 20 years. Most of the building stock has been exposed to severe seismic forces and a great amount of seismic energy in recent earthquakes, such as 1999 Kocaeli, 2011 Van, 2020 Izmir and 2023 Kahramanmaraş earthquakes [1-3]. It follows that they will either collapse or suffer damage if this energy surpasses the lateral bearing capacity due to their inadequacy to operate in a safe manner, particularly in relation to the functional performance criteria. During the last several decades, many scientists have examined creative and attractive protection mechanisms of structure to improve the energy dissipation ability or to reduce structural seismic damages [4-6]. The innovative method for controlling structural vibration during earthquake ground motion can be divided into three systems: base isolation system (BIS), active control system (ACS), and passive energy dissipation system (PEDS) [7-10]. In consequence of this, the construction will eventually weigh less and be built at lower expenses.

It is important to reduce the damage that may occur following an earthquake, which imposes many injuries, casualties, and significant structural damage. Therefore, retrofitting insufficient structural elements (e.g., beam, column, etc.) of old buildings is necessary in structural engineering. During and immediately after an earthquake, some buildings, such as hospitals and important state houses, must keep functioning and be in full operation. This can only be achieved by using the energy dissipation systems (EDSs) [11]. EDSs may be classified such as active, passive, semi-active, and hybrid (consists of both active and passive) mechanisms. Both the dampers and the BIS are considered passive devices, and are widely used by structural designers because (i) they do not need external energy, (ii) there is no need for maintenance throughout functioning, (iii) they have a cost-benefit in the long term and (iv) they are easy to apply [12, 13].

Base Isolation

BI technology is a remarkable method applied worldwide for multi-storey buildings. However, they may have some limitations on applications due to significant technical and economic issues. The implementing BI technology becomes simple and inexpensive for newly constructed structures, but it requires excavation and temporary support work for those that already exist [14]. It has become increasingly popular for seismic retrofitting existing buildings for the past two decades due to reducing the seismic effects on the structure [15, 16]. The concept of BI depends on disconnecting the building from the ground and connecting the BI to the building itself and it is widely used to decrease inter-story drifts, story accelerations and story displacements [17]. Two types of BI technology are typically used in the literature, i.e., sliding mechanisms and elastomeric bearings. The elastomer bearings are developed to mitigate lateral seismic effects by offering a layer with less lateral stiffness. The sliding systems aim to mitigate seismic loads by permitting frictional slide and reducing the quantity of shear transfer [18, 19]. In most cases, structural engineers adopt three different kinds of elastomer bearings for the building: (i) lead rubber bearings (LRBs), (ii) natural rubber bearings and (iii) high-damping rubber bearings [20, 21].

Lead Rubber Bearings (LRBS)

The LRB isolation system was used in this research, and the LRB's hysteretic behavior and typical configuration were given in Figure 1. This system is made up of many rubber layers as well. Steel lead core inserted in the center of the rubber as illustrated in Figure 1a. The LRB hysteresis loop is represented as a bilinear curve, where k_{eff} is the effective stiffness, k_u and k_d are the initial elastic and the post-yield stiffnesses of the bearing, respectively. F_y and d_u are the yield strength and yield deformation of the bearing, respectively. F_{max} and d_i are the maximum force and displacement of the bearing, respectively, as depicted in Figure 1b.

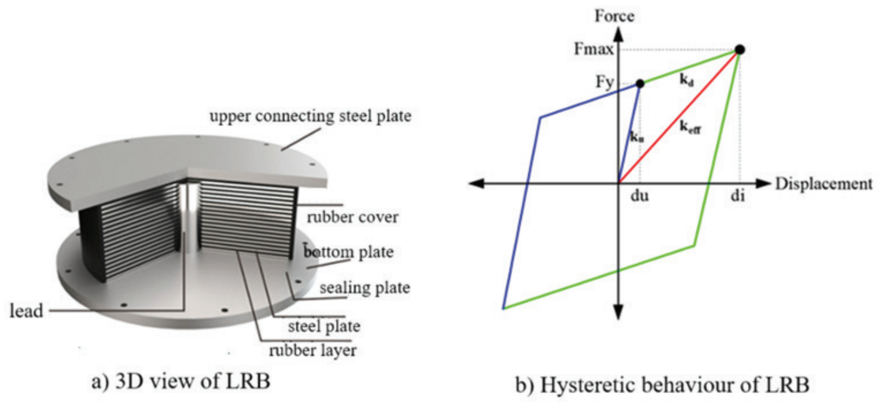

Figure 1. The view of structural details and the mechanics of the LRB.

The LRBs are essential elements in elastomer-based isolation technologies. In such bearings, the rubber allows lateral flexibility to have a longer service life cycle, while the lead core inside the rubber releases energy during the cyclic movement of the seismic motion [22]. One of the main characteristics of LRB is that it has a high vertical stiffness so it can carry a substantial vertical load and can move laterally with relatively lower horizontal stiffness [23, 24]. The LRB can alter a building's natural period due to its high flexibility, preventing resonance in the structure exposed to seismic vibrations. Also, the LRB can support the structural system vertically, allowing a lateral displacement and boosting the system's damping to the appropriate value [24]. There are several studies about the behavior of LRB-isolated buildings under the seismic movements [25-27]. For instance, Ren et al. [28] used computational and empirical approaches to study the LRB's compressive force with different shape variables. Sesli et al. [29] compared the impacts on a seismically isolated and fixed base building of far, near, and pulse-type ground motions. Bhandari et al. [30] examined the RC building's seismic performance, which is separated with LRB, using the capacity spectrum methodology and concluded that this method was accurate in predicting the maximum values of the BI frames as much as 0.2g. Chanda and Debbarma [31] developed fragility curves to assess the dynamic behavior of LRB-isolated multi-story RC frames under far-field and near-field seismic waves. Mousazadeh, et al. [32] studied an optimization approach to decrease the LRB's lifetime cost. Ye et al. [33] suggested a seismic design based on displacements for analyzing multi-story LRB-building systems using response spectrum approaches and they obtained that seismic responses were within 10% of the specified values. Santhosh et al. [26] and Haque et al. [25] confront the effects of the LRB with the fixed base building under seismic forces they obtained that the LRB base-isolated building was reduced the top story horizontal displacement and acceleration, and both the base shear and the floor's drift were lower for LRB base-isolated building. Choun et al. [34] studied the impact of alterations to the LRB's mechanical characteristics on seismic behavior and concluded that mechanical property changes in the isolator had a substantial impact on the isolator's shear strain and the superstructure's acceleration response. Kanbir et al. [35] compared multi-story frames with LRB base-isolated building exposed to NF seismic waves. The majority of LRB researches (i.e., Bhandari et al. [30], Chanda and Debbarma [31], Mousazadeh et al. [32], Wang et al. [36]) has focused on the effectiveness of the BI methodology to decrease structural seismic effects in the event of a dynamic force. Thus, BI system can lead to excessive displacements and undesirable conditions due to the inherent behaviour of the isolation material for buildings placed in adjacent or narrow locations [37]. However, it is becoming increasingly common in engineering applications to use supplemental damping devices (e.g., fluid viscous dampers (FVDs)) and LRB systems together to overcome those worst scenarios and control the structural seismic responses [38].

Viscous Dampers

Viscous dampers (VDs) are one of the PED devices, and they can be applied to the new or existing structure to control the building's seismic response. The widespread acknowledgment of viscous dampers in the literature is attributed to their capacity for operating out of phase with structural forces and their non-interference with the stiffness of a building system. They are made of highly resistant materials, and the silicone-based fluid that circulates between the piston and cylinder arrangement absorbs or dissipates energy that is imparted by the piston [39]. In this study, VDs were used to dissipate energy. Mechanical details and force-displacement relationship of VD are given in Figure 2 [40].

Politopoulos [41] revealed that viscous dampers efficiently reduce the isolator displacement and the floor acceleration close to the first mode. Higher modes, on the other hand, have a substantially greater impact on floor acceleration. Boksmati et al. [42] investigated the effect of soil conditions on the energy dissipation of bare frame and BI frame system having viscous dampers exposed to seismic loading and it was obtained that the BI frame was less influenced by the type of soil. Chang et al. [43] conducted shake table tests and developed an analytical model to analyse three-story steel buildings that had been modified with viscous dampers. In the case of El Centro earthquake striking the

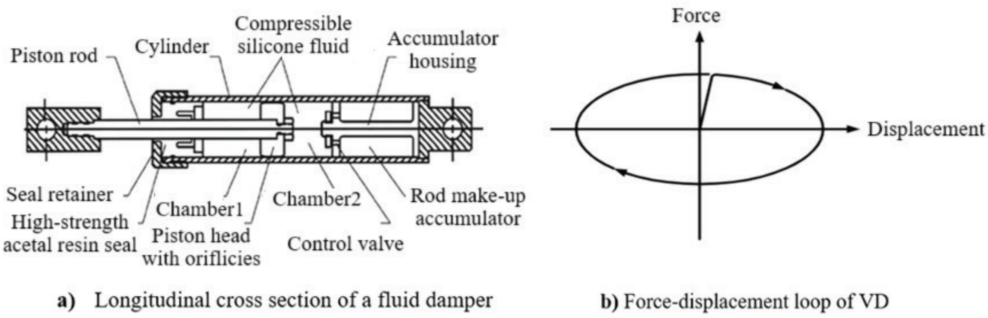

Figure 2. The view of structural details of VD.

building, where viscous dampers were applied, it resulted in 68% and 30% reduction in the story displacement and shear force, respectively. Hwang et al. [44] proposed an equation, including the combined effects by considering the phase angle between the LRB and viscous damper, and the displacement of the isolation system. Ganji and Kazem [45] compared seismic behaviors of buildings with 5, 10 and 15 stories equipped with LRB or viscous dampers under the NF seismic movements.

Viscous dampers with proper damping coefficient selection significantly improve the dynamic response of structures [46-50]. Domenico and Ricciardi [51] provided a dynamic configuration that consisted of the BI system and with a tuned-mass-damper situated in the building's basement. Yaktine et al. [52] examined the combined responses of LRB or viscous dampers having irregular plan RC buildings with 3-story, 8-story, and 20-story. Hatipoglu and Duzgun [53] investigated the dynamic response of adjacent buildings with different VD distribution along building height considering soil-structure interaction. Thakur and Tiwary [54] investigated the seismic responses combined with LRB and viscous dampers. They concluded that the combined system significantly improved the behavior of the structure.

An existing MDOF building (at Keio University in Japan) with different LRBs stiffnesses, and the same building with and without viscous dampers installed in the basement level were investigated in this study. For this purpose, three different stiffness ratios (i.e., the sum of the stiffnesses of the first-floor columns (k_1) to the sum of the stiffnesses of LRB (k_b); k_1/k_b=20, 40 and 80) were chosen to assess the effect of LRBs' stiffness on the seismic response of the building. The ratio k_1/k_b=20 is obtained by dividing B1F by B2F in Table 4. The remaining two ratios (k_1/k_b=40 and 80) are assumed, considering the potential reduction in stiffness of LRB during the lifespan of the building being studied. In addition, to investigate the effects of supplemental VD on the seismic response of the building, six different damping coefficients were adopted. One of the damping coefficients used by Dan and Kohiyama [55] is employed as a base to derive various coefficients by scaling them with different factors. The building model was developed in MATLAB language [56] and verified with experimental results of Kohiyama et al. [57].

NUMERICAL STUDY

Details of the Sosokan Building

Today, the base-isolation systems with low stiffness are available in many Japanese buildings. The Sosokan building, which has elliptical tower at the main gate to the campus, was also constructed in 2000 at Keio University, Japan, as illustrated in Figure 3a [57, 58]. During the 2011 Great East Japan earthquake, the building acted as a passive base isolation system as the semi-active system was out of service for maintenance work. It was observed following the earthquake that only slight damage was detected in the RC building adjacent to the Sosokan and additionally the building response in Sosokan was effectively mitigated by its base isolation system [55].

In the building with EDS, a total of 32 passive viscous dampers installed base layer of the building. Structural member details of the building were given in Table 1, while the LRB details were given in Table 2 [57]. Figure 3b depicted the isolation layer plan of the building, and in the isolation layer 65 laminated rubber bearings were used. 16

Table 1. The structural member details

Member	Type of material	Type of geometry
Girders	Steel	H-(1000-600) × (300-200) × (12-22) × (19-40)
Columns	Steel,	B × D =1000 × 1000
	Steel-RC,	Ø600, Ø550, Ø450
	Concrete-filled steel tubes	

Table 2. The LRB properties

Property	Isolator diameter				
	Ø1000	Ø900	Ø800	Ø700	Ø600
The number of isolators	8	10	15	20	12
Thickness and number of rubber layers	7.5mm-26	6.8mm-26	6.0mm-26	5.3mm-26	4.5mm-33
Thickness and number of steel plates	4.5mm-25	4.5mm-25	4.5mm-25	4.5mm-25	3.2mm-32
Upper and lower steel flanges	33mm- Ø1450	32mm-Ø1300	30mm-Ø1200	25mm-Ø1050	25mm-Ø900
Anchor bolts	8-M42	8-M36	8-M36	8-M33	8-M33

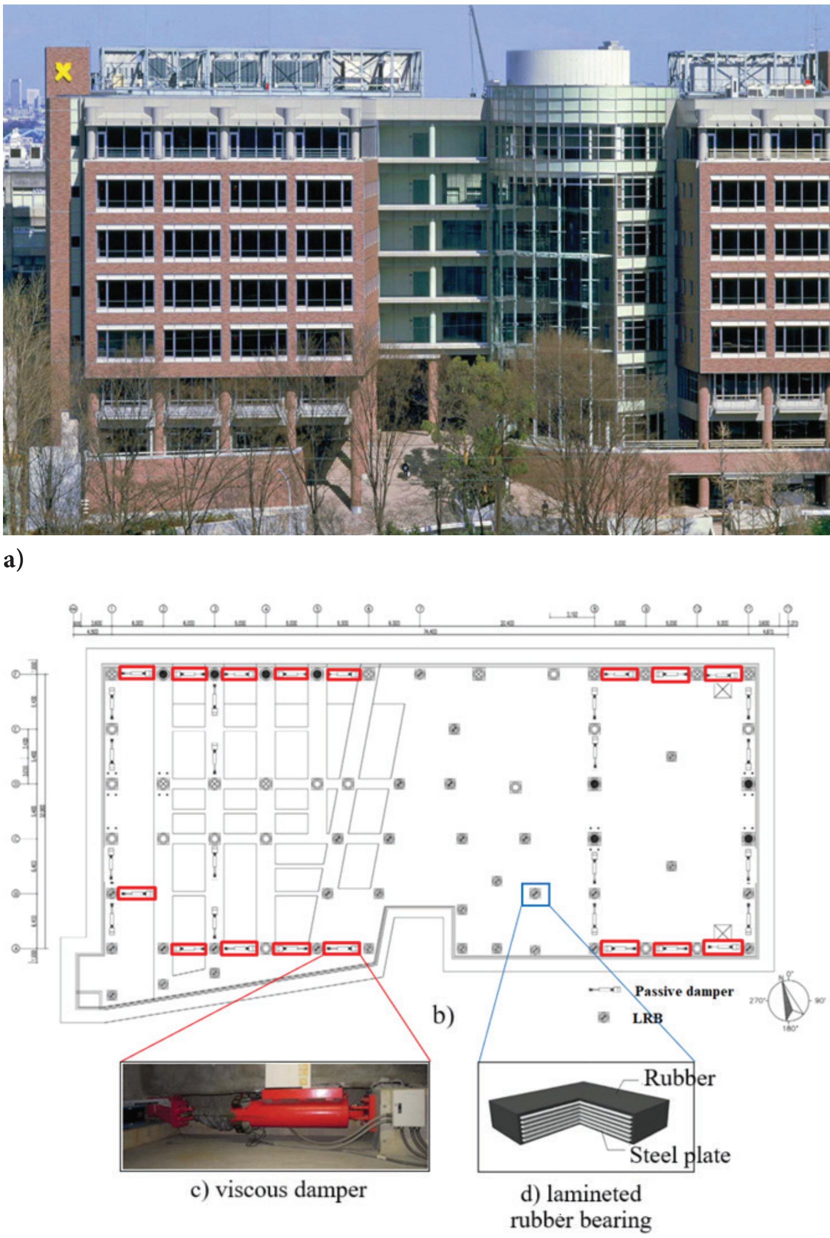

Figure 3. a) The Sosokan building in Japan, **b)** Isolation layer plan, **c)** The viscous damper installed in the building's isolation layer, and **d)** The cross-section of LRB.

passive viscous dampers installed in both the EW and NS directions were utilized. The passive viscous dampers in the EW direction were shown in red rectangles, while the LRB devices were shown in blue rectangle. The passive viscous dampers and LRB illustrations, which were placed in the building's base layer, were shown in Figure 3c-d.

This building had seven floors and two basement floors for a total of nine floors The section detail of the building center line in the short axis direction was shown in Figure 4 [57]. The building structure was made of a combination of steel, steel-reinforced concrete, and concrete-filled steel tubes. For more detailed information about the building isolated system equipped with dampers, see the work of Kohiyama et al. [57].

Mathematical Model of the Sosokan Building and Formulation

In the study, a two-dimensional model of the building, which consists of one-basement floors, seven normal floors, and a roof floor (B1F + 7F + RF), is used in the dynamic analysis. B2F, B1F,1F and RF represent the 2nd basement floor, 1st basement floor, 1st floor, and roof floor, respectively. The considered building model is shown in Figure 5. The isolation layer, which is installed in B2F, is consists of 65 LRBs and 16 passive viscous dampers in EW direction.

Sigma J Eng Nat Sci, Vol. 43, No. 1, pp. 301–315, February, 2025

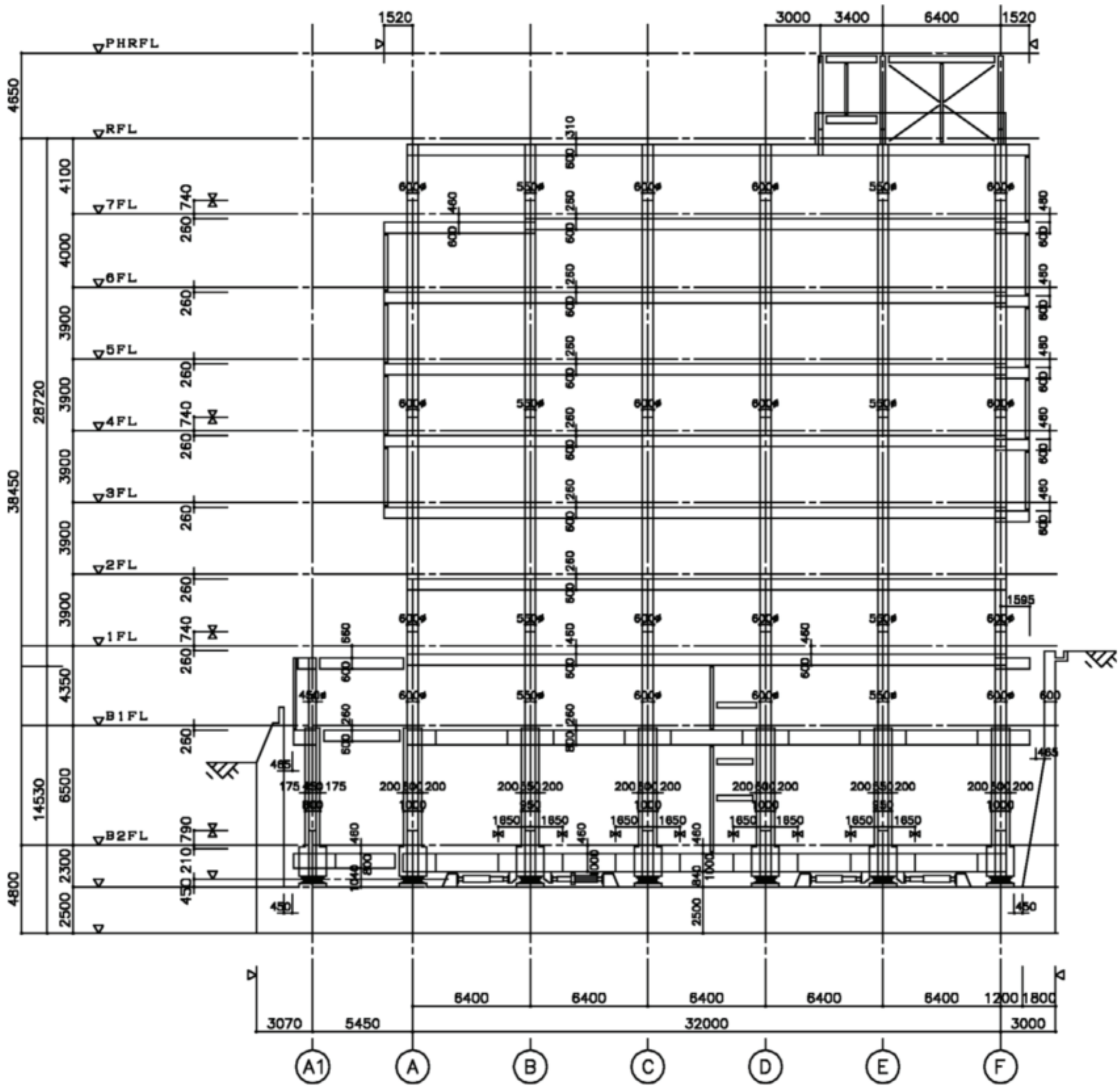

Figure 4. The section detail of the building center line in the short axis direction.

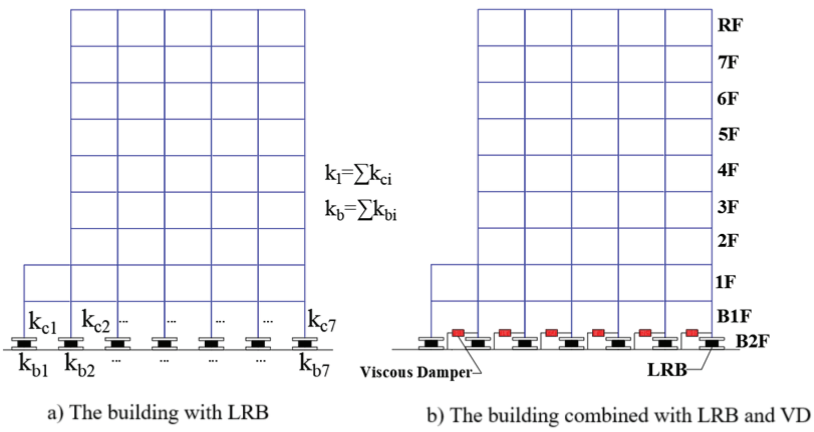

Figure 5. Two-dimensional model of the Sosokan building drawn by using Figure 4.

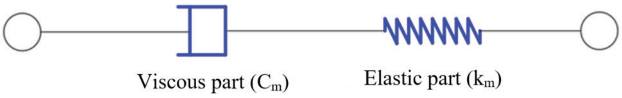

Figure 6. Maxwell model of the VD

In Figure 5, k_{ci} (i = 1,2,…,7) is the total stiffness of the ith column in the frame depth, while k_{bi} (i = 1,2,…,7) is the total stiffness of the ith LRB in the frame depth In the study, Maxwell type viscous damper modelling is used as recommended Kohiyama et al. [57], and its mathematical model is given in Figure 6.

- In the study, to investigate the building having only a BI (Base Isolation) system with different LRB stiffnesses (for the case shown in Figure 5a**),** three different stiffness ratios (k_1/k_b) were chosen, and these ratios were 20, 40, and 80. k_1 is the total stiffness of all 1st basement floor columns (B1F). k_b is the total stiffness of all LRBs on the 2nd basement floor (B2F). Note that there is no change in the total stiffness of columns on the 1st basement floor (B1F); instead, only the total stiffness of LRBs on the 2nd basement floor (B2F) is changed by a ratio.
- The building, which had both a BI system (i.e., the stiffness ratio of k_1/kb = 80 is taken) and viscous dampers, which had six different damping coefficients (shown in Table 3) at B2F level, was also investigated (for the case shown in Figure 5b).

The equation of motion of the system is formulated as follows (as given in Kohiyama et al. [57])

$$M\ddot{x} + C\dot{x} + Kx = Eu + F\ddot{z} \quad (1)$$

where M, C, and K are the mass, damping, and stiffness matrices of the structure, respectively. x, $\dot{x}$ and $\ddot{x}$ are the displacement, velocity, and acceleration vectors of the structure. u and $\ddot{z}$ are the damping force of viscous dampers in isolation layer and ground acceleration, respectively. The E is a vector matrix, which indicates the location where the damping forces apply. The vector F shows the mass matrix for seismic force calculation.

The matrices and vectors in Eq. 1 are rearranged as follows:

$$M = diag\left[m_1, m_2, ..., m_{10}\right] \quad (2)$$

$$C=\begin{bmatrix} c_1+c_2 & -c_2 & \cdots & 0 & 0 \\ -c_2 & c_2+c_3 & \cdots & 0 & 0 \\ \vdots & \vdots & \ddots & \vdots & \vdots \\ 0 & 0 & \cdots & c_9+c_{10} & -c_{10} \\ 0 & 0 & \cdots & -c_{10} & +c_{10} \end{bmatrix} \quad (3)$$

$$K=\begin{bmatrix} k_1+k_2 & -k_2 & \cdots & 0 & 0 \\ -k_2 & k_2+k_3 & \cdots & 0 & 0 \\ \vdots & \vdots & \ddots & \vdots & \vdots \\ 0 & 0 & \cdots & k_9+k_{10} & -k_{10} \\ 0 & 0 & \cdots & -k_{10} & +k_{10} \end{bmatrix} \quad (4)$$

$$x=\left[x_1 \quad x_2 \quad \cdots \quad x_{10}\right]^T \quad (5)$$

$$E=\left[1 \quad 0 \quad \cdots \quad 0\right]^T \quad (6)$$

$$F=\left[-m_1 \quad -m_2 \quad \cdots \quad -m_{10}\right]^T \quad (7)$$

where m_i, c_i, k_i are the mass, damping and spring stiffness parameters of each floor, respectively, for i = 1, 2, 3, …,10 while x_i is horizontal displacement of each floor relative to ground motion. The structural parameters of m_i, c_i, k_i were given in Table 4 [55]. These parameters are also used for the verification of the Sosokan building model in MATLAB language.

Table 3. The passive damping coefficients used in this study

Abbreviation	Damping Coefficient ($x10^6$ Ns/m)
Cd_1	**1.4**
Cd_2	**2.8**
Cd_3	**5.6**
Cd_4	14
Cd_5	210
Cd_6	560

Table 4. Parameters of the building (E-W direction)

Floor	Mass ($x10^6$ kg)	Stiffness ($x10^9$ N/m)	Damping ($x10^6$ Ns/m)
RF	2.4999	0.9623	6.2245
7F	2.0664	1.2022	7.7761
6F	2.0371	1.4772	9.5550
5F	2.0369	1.8068	11.6870
4F	2.0500	2.1536	13.9296
3F	2.0331	1.9747	12.7729
2F	1.8264	2.1377	13.8269
1F	2.4906	2.9290	18.9455
B1F	3.4382	2.2320	14.4368
B2F	4.9814	0.1042	0

From Eq. 1, velocity vector of the structure ($\dot{x}_t$) is defined as below

$$\dot{x}_t = Ax_t + Bu + D\ddot{z} \quad (8)$$

where,

$$x_t = \begin{bmatrix} x \\ \dot{x} \end{bmatrix},\ A = \begin{bmatrix} O_{10x10} & I_{10x10} \\ -M^{-1}K & -M^{-1}C \end{bmatrix},\ B = \begin{bmatrix} 0_{10x1} \\ M^{-1}E \end{bmatrix} \text{ and } D = \begin{bmatrix} 0_{10x1} \\ M^{-1}F \end{bmatrix} \quad (9)$$

The Maxwell-type viscous damper model for the building system, the velocity equation is defined as follow

$$\dot{x}_m = A_m x_m + B_m \tilde{u}_S + D_m \ddot{z} \quad (10)$$

where $\tilde{u}_S$ refers to the control force of passive viscous damper. From Eq. 10,

$$x_m = \begin{bmatrix} x_t \\ \dot{x}_d \end{bmatrix} = \begin{bmatrix} x \\ \dot{x} \\ \dot{x}_d \end{bmatrix},\ A_m = \begin{bmatrix} A & -B \\ k_d B_u & -k_d/c_d \end{bmatrix},\ B_m = \begin{bmatrix} B \\ 0 \end{bmatrix} \text{ and } D_m = \begin{bmatrix} D \\ 0 \end{bmatrix} \quad (11)$$

where c_d, k_d and x_d denote damping coefficient, stiffness and displacement of the passive viscous damper, respectively. B_u is stated as matrix form as below

$$B_u = \begin{bmatrix} 0_{1x10} & 1 & 0_{1x9} \end{bmatrix} \quad (12)$$

To model and simulate the building in MATLAB-R [56], the "ss" command, which creates a state-space model with given properties, and the "*lsim*" command, which plots the simulated time response of the model, are employed. In the study, in the base isolated model (i.e., nine-story building with isolation layer), the matrix size of the mass (M), damping (C), and stiffness (K) in Eq. 9 is a twenty-by- twenty (20*x*20).

The BI system equipped with viscous damper (BI&VD1) refers to base isolation with installed viscous damper coefficient $C_d = 1.4x10^6$ *Ns/m* in the isolation layer (i.e., nine-story building with both having BI and installed VDs at the same level). Eq. 10, which includes the Maxwell-type viscous damper model, is used for the model. The model has a twenty-one-by-twenty-one (21*x*21) matrix size in mass (M), damping (C), and stiffness (K). Total passive viscous damper stiffness k_d is calculated and Kohiyama [55] as $47.0381x10^7$ *N/m*.

The Verification of the Building Model

It is necessary to verify the code written in MATLAB before executing building simulation. Based on the above given structural details and equations, the mathematical model of the Sosokan building (having 65 LRB and 16 supplemental VDs) was written in MATLAB. The building model was subjected to the Tohoku earthquake (as given in Table 5 and Figure 7) [59].

The building model was verified by plotting acceleration time history results obtained from this study and the results given by Kohiyama et al. [57] and Dan and Kohiyama [55]. The acceleration time history of 7th floor (7F) is obtained by using Eq. 10 and the data in Table 4 and Table 5, and these results were given in Figure 8 for comparison. Figure 8a shows the results from this study, while Figure 8b shows the results of Kohiyama et al. [57]. In the results of Kohiyama et al. [57], the time-history responses of the model with

Table 5. The ground motion record in the study

Earthquake	Year	Mw	Station ID	Component	PGA (g)
Tohoku	2011	9.1	Tohoku	E-W	0.711

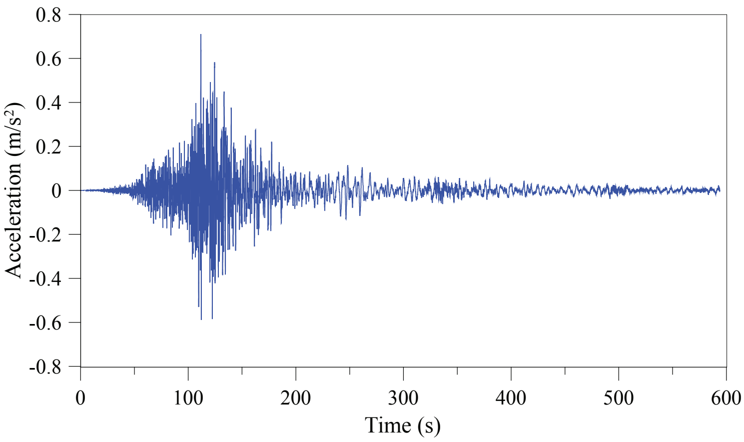

Figure 7. The time history record of 2011 Tohoku earthquake.

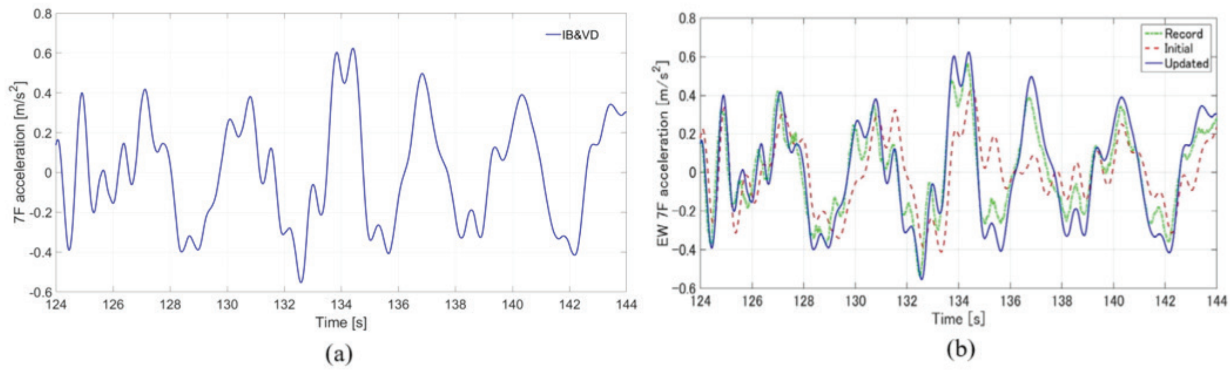

Fig. 8 (**a**) The results of this study of the BI&VDs model, (**b**) The results of Sosokan building of the BI&VDs model Kohiyama et al. [57] ("updated").

"updated" structural parameters based on system parameters identification were illustrated with blue colour line. It is apparent that the results obtained from both studies are the same.

RESULTS AND DISCUSSION

Base Isolation (BI) Model

The building model with three different LRB stiffnesses (k_1/k_b) was simulated under the Tohoku earthquake to discuss the effect of LRBs' stiffness on the seismic performance of the building. The results were obtained for the case where the sum of the stiffnesses of the first-floor columns (k_1) and the sum of the stiffnesses of the base isolation (k_b) were 20, 40, and 80. It was obtained that various LRB stiffnesses brought about different isolation layer displacements in the building, as illustrated in Figure 9. For the case the stiffness ratio (k_1/k_b) equals 20, the maximum displacement in the isolation layer was obtained as 45.2 cm, which was the smallest displacement among the cases considered in this study. The largest drift in the isolation layer (B2F), which is 93.4cm, was obtained at the stiffness ratio (k_1/k_b) of 80 (i.e., when the total stiffness of the LRB was the smallest). Also, for the case the stiffness ratio (k_1/k_b) equals 40, the displacement of the isolation layer was 56.2cm. As can be seen in Figure 9, the larger the stiffness ratio (k_1/k_b), the smaller the drift occurred at the above levels (from B1F to RF). The obtained results were reasonable because the small LRB stiffness in the isolation layer (B2F) resulted in large base displacement and allowed the above floors to move together without causing large inter-story drifts.

Figure 10 depicted the 7th floor (7F) time-history acceleration of the building. The maximum acceleration for the considered cases were also shown in Figure 10. The bigger the ratio (k_1/k_b) was, the smaller the maximum acceleration observed. To put it differently, the maximum acceleration at the above floors was lessened as the stiffness of the LRB was reduced. It was reasonable to say that the smaller drift the above levels (B1F, 1F, 2F, etc.) had, the smaller maximum acceleration the building experienced.

The Base Isolated Building Equipped with Viscous Dampers (BI&VDS)

The building model with a stiffness ratio (k_1/k_b) of 80 was equipped with sixteen passive viscous dampers

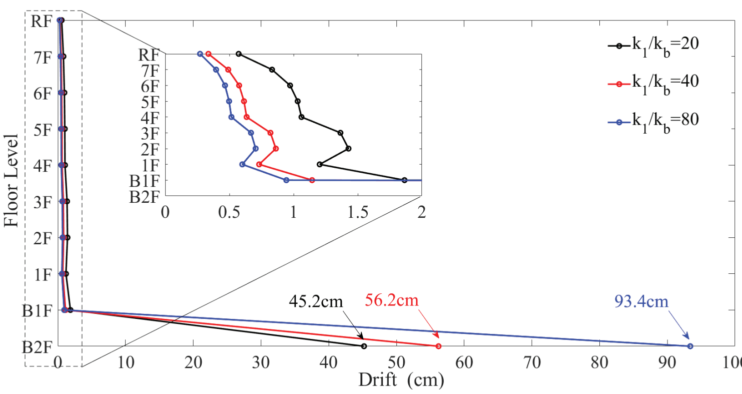

Figure 9. The maximum inter-story drifts for different LRB stiffnesses under the Tohoku earthquake.

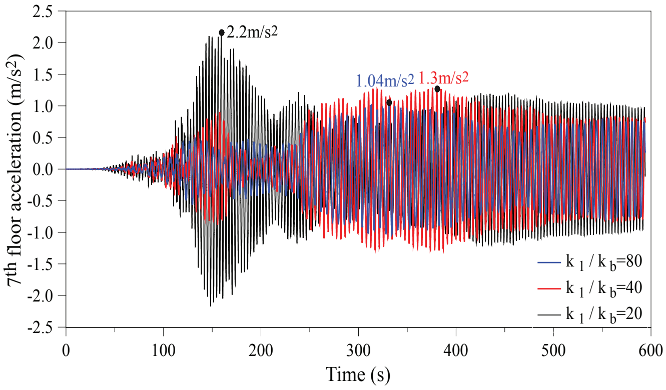

Figure 10. The time history acceleration of 7th floor (7F) for different LRB stiffnesses under the Tohoku earthquake

installed in the E-W direction in the base isolation layer (B2F). The seismic responses of the building for the case of base isolation (BI) and for the base isolation equipped with viscous dampers (BI&VDs) are given in Figure 11. The largest displacements occurred on the 2nd basement floor (B2F) in all cases. In addition, the BI system (no viscous damper) had the largest displacement (93.4 cm) among the seven model simulations. By VD instalments, a significant decrease in inter-storey drifts was observed at B2F level, where the isolation layer is located. For the case of high damping coefficient assignments, the inter-storey drifts in the 2nd basement (B2F) are reduced, yet once the damping coefficient was significantly increased (e.g., VD5 and VD6), the inter-story drift at above levels (from B1F to RF) are also increased. This showed that a proper damping coefficient assignment was needed for multi objective optimization (i.e., reducing both drift and acceleration).

Figure 12 illustrated the 7th floor time-history acceleration of BI (no VDs) and BI&VDs models with a stiffness ratio of 80 for different damping coefficients of viscous dampers (from VD1 to VD6), and the values of maximum acceleration for the considered cases were also shown in Fig. 12. Once the dynamic response of the BI&VDs (from VD1 to VD6) model was compared with the BI model, it was observed that the maximum acceleration of the building was generally reduced when viscous dampers were added to the BI building model. However, the damping coefficient of VD6 increased the maximum acceleration at above level (e.g., 7F). A similar discussion was done for Fig. 11. This showed that large damping coefficient assignment (e.g., VD6) could increase the maximum acceleration of the building even though it reduced the drift.

To assess the response of the BI&VDs model, the viscous damper's hysteresis loop is depicted in Fig. 13. Regarding that, the force-drift loops were given for different damping coefficients. The total damper force represents the total force of the 16 viscous dampers in the building. The damper force slightly increased as the damping coefficient increased from the cases of VD_1 to VD_4 (except VD_5 and VD_6). However, a large amount of damper force was required for the cases of VD_5 and VD_6 compared with the other four VDs.

The total damper energy dissipated by 16 viscous dampers in the building versus time was shown in Figure

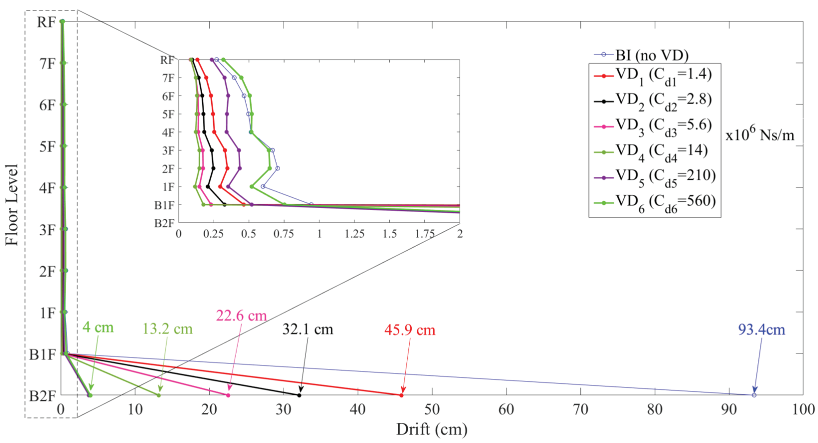

Figure 11. The inter-story drift results for the BI (no viscous damper) and BI&VDs models with a stiffness ratio (k_1/k_b) of 80 for different damping coefficients-under the Tohoku earthquake.

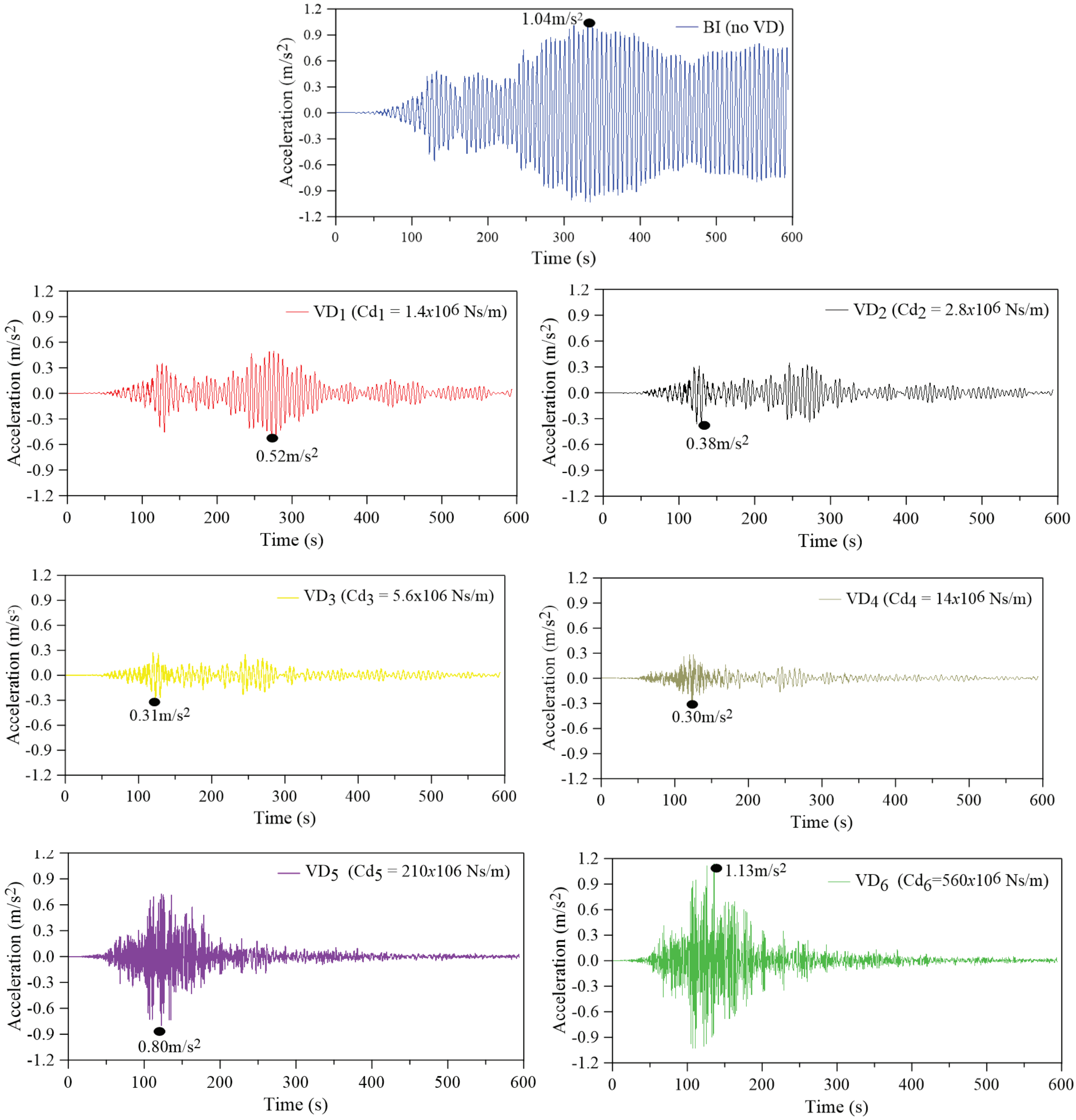

Figure 12. The maximum time history acceleration of 7th floor for the BI and BI&VDs models with a stiffness ratio of 80 for different damping coefficients-under the Tohoku earthquake.

14. The largest damper energy was observed in the case of VD_1, while the smallest damper energy was obtained in the case of VD_6. It was obtained that as the damping coefficient increased (from VD1 to VD6), the maximum energy dissipation dropped.

The seismic responses of the building in the case of the BI (no VDs) and the BI model equipped with 16 viscous dampers (BI&VDs) were summarized in Table 6. As compared to the BI system, the maximum displacement at the B2F level in the use of viscous dampers reduced by up to 96%, while the maximum acceleration of 7th floor reduced by up to 71%. However, even though BI&VD_6 model reduced the maximum displacement of the 2nd basement floor by 96%, it increased the maximum acceleration of the floor by 8.7%. It appears that a large VD coefficient at the base isolation layer (B2F) does not reduce acceleration.

The effects of LRB stiffness were examined by employing linear time-history analysis, both with and without

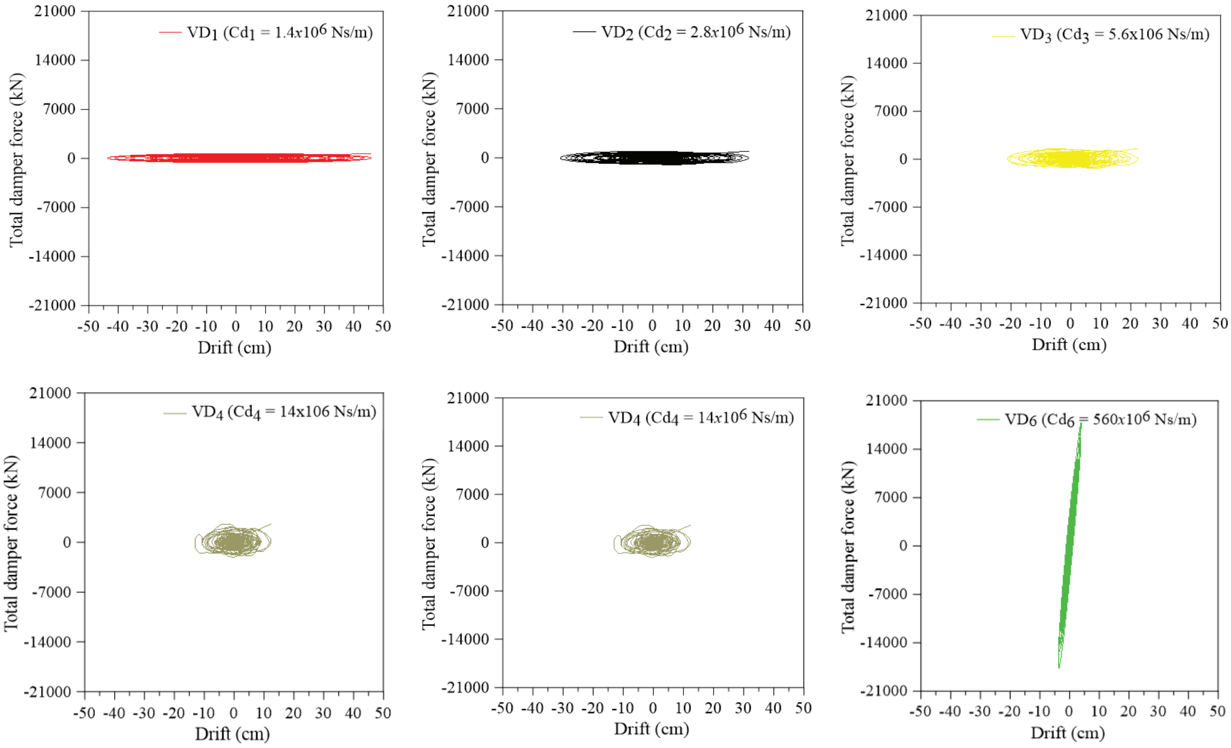

Figure 13. Hysteresis loop of the total damper force for six different damping coefficients-under the Tohoku earthquake.

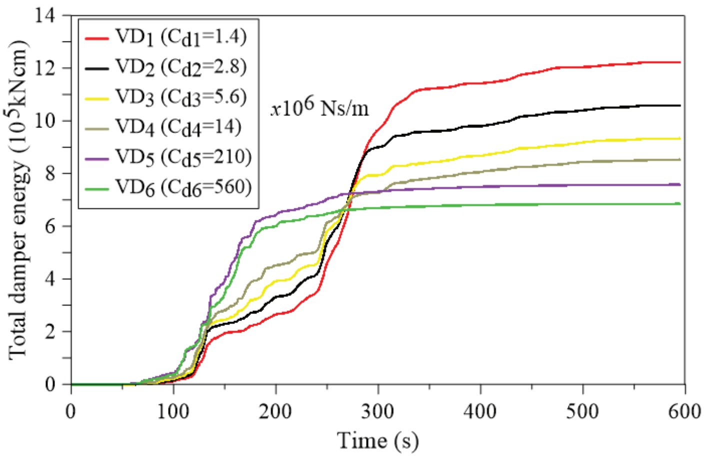

Figure 14. The dissipated energy by 16 VDs versus time for six different damping coefficients-under the Tohoku earthquake.

Table 6. Main results of different models subjected to the Tohoku earthquake (Δ=reduction)

Building model	Max. displ. in 2nd basement floor (cm)	Δ	Max. acceleration in 7th floor (cm/s²)	Δ
BI	93.4	-	104	-
BI&VD$_1$	45.9	-51%	52	-50%
BI&VD$_2$	32.1	-66%	38	-63%
BI&VD$_3$	22.6	-76%	31	-70%
BI&VD$_4$	13.2	-86%	30	-71%
BI&VD$_5$	4.0	-96%	80	-23%
BI&VD$_6$	3.8	-96%	113	**+8.7%**

viscous dampers on the displacement of the isolation layer, inter-story drift, and acceleration of the building.

CONCLUSION

The present study represents an analytical investigation of a benchmark Japanese 9-story Sosokan building. The building originally had a base isolation system consisting of 65 LRBs and 16 passive viscous dampers in the EW direction. The building was modeled using the MATLAB language, and the building model was verified by generating the experimental results of Kohiyama, et al. [52]. To assess the effects of LRBs' stiffness on the seismic performance of the building, three different stiffness ratios were chosen, and to obtain those, the 2011 Tohoku earthquake was used for each model. It was examined the effect of lead rubber bearings's (LRBs) stiffness both with and without supplemental viscous dampers (VDs) on the seismic reactions of buildings. Also, the variation of the seismic response was investigated in case of the building has both a base isolation (BI) system and viscous dampers (BI&VDs) with different damping coefficients. To evaluate the effect of different LRB stiffnesses and viscous damper coefficients on the seismic response of the building, each building model was subjected to the Tohoku earthquake. Based on the results of the analyses, the following conclusions can be drawn:

- Among the three (k_1/k_b) ratios (20, 40 and 80), the value of 80 experienced the largest displacement at 2nd basement floor, however it resulted in the smallest drift and acceleration at the above levels (from 1st basement floor to roof floor) compared with the ratios of 20 and 40. These findings confirmed that large stiffness ratio (k_1/k_b), i.e. the small LRB stiffnesses, is directly associated with large displacement at the base isolation level, and small acceleration and inter-story drift at the above levels.
- The displacements and accelerations at 2nd basement floor and above levels significantly reduce in the LRB base isolated system equipped with viscous dampers (BI&VDs) as compared to BI (no VDs) model. Although a higher damping coefficient of viscous damper (e.g., VD_6) reduces the maximum displacement at 2nd basement floor level, it increases the acceleration of the building and reduces its energy dissipation capacity. Therefore, an obvious finding emerging from this study is that to achieve multi-objective optimization (i.e., reduction of both displacement and acceleration at the same time) for the building's seismic response, a proper damping coefficient (C_d) is needed.
- It is obtained that the maximum displacement at the 2nd basement floor in the use of viscous dampers reduces by up to 96%, while the maximum acceleration of top floor reduces by up to 71%. Also, it appears that the using a large VD coefficient at the base isolation layer (2nd basement floor) does not reduce acceleration.
- The study's findings indicate that blindly adding damping coefficients could lead to increased structural displacements in the upper levels (above isolation stories) and, consequently, increase the system's acceleration. This could result in unnecessary costs and potential damage to acceleration-sensitive equipment in the building.

Future Study

Further research should focus on determining an optimal damping coefficient at a building's base isolation level for the sake of multi-objective optimization of building seismic performance. It would be beneficial to expand the study to include low-, medium-, and high-rise buildings.

ACKNOWLEDGEMENTS

The first author, Adnan, expresses profound gratitude to Professor Masayuki Kohiyama for providing supplementary numerical data pertinent to this study following the first author's visit to Keio University in Japan in 2019.

AUTHORSHIP CONTRIBUTIONS

Authors equally contributed to this work.

DATA AVAILABILITY STATEMENT

The authors confirm that the data that supports the findings of this study are available within the article. Raw data that support the finding of this study are available from the corresponding author, upon reasonable request.

CONFLICT OF INTEREST

The author declared no potential conflicts of interest with respect to the research, authorship, and/or publication of this article.

ETHICS

There are no ethical issues with the publication of this manuscript.

REFERENCES

[1] Tonyali Z, Alemdağ EL, Kibar GT. Evaluation of Seismic Response of the Cross-Laminated Timber (CLT) Multi-Storey Residential Building Under the February 6, 2023, Kahramanmaraş Earthquakes. J Architect Sci Appl 2024;9:41–63. [CrossRef]

[2] Yurdakul M, Yılmaz F, Artar M, Can Ö, Öner E, Daloğlu AT. Investigation of time-history response of a historical masonry minaret under seismic loads. Structures 2021;30:265–276. [CrossRef]

[3] Tonyali Z, Kiral A. Evaluation of Earthquake-Related Damages on the Reinforced Concrete Buildings due to the February 6, 2023, Kahramanmaras-Turkiye Earthquakes. Recep Tayyip Erdoğan Üniv Fen Mühendislik Bilim Derg 2024;5:89–114. [CrossRef]

[4] Kiral A, Gurbuz A. Using supplemental linear viscous dampers for experimentally verified base-isolated building: Case study. J Struct Eng Appl Mech 2024;7. [CrossRef]
[5] Kiral A, Tonyali Z, Ergün M. A comprehensive analysis of the ground motions of the 2023 Kahramanmaraş, Türkiye earthquakes. Earthq Struct 2025;26:203–219.
[6] Altunisik AC, Sesli H, Husem M. Effect of near-fault ground motion with pulse signal on dynamic response of dam-reservoir-foundation systems. Građevinar 2022;74:1059–1086. [CrossRef]
[7] Soong T-T, Spencer Jr BF. Supplemental energy dissipation: state-of-the-art and state-of-the-practice. Eng Struct 2002;24:243–259. [CrossRef]
[8] Güneyisi EM, Deringöl AH. Seismic response of friction damped and base-isolated frames considering serviceability limit state. J Construct Steel Res 2018;148:639–657. [CrossRef]
[9] Kahya V, Onur A. A sequential approach based design of multiple tuned mass dampers under harmonic excitation. Sigma J Eng Nat Sci 2019;37:225–239.
[10] Ahmadi G. Overview of Base Isolation, Passive and Active Vibration Control Strateies for a Seismic Design of Structures. Sci Iran 1995;2.
[11] Shang Q, Wang T, Li J. Seismic fragility of flexible pipeline connections in a base isolated medical building. Earthq Eng Eng Vibrat 2019;18:903–916. [CrossRef]
[12] Spencer Jr BF, Nagarajaiah S. State of the art of structural control. J Struct Eng 2003;129:845–856. [CrossRef]
[13] Aliakbari F, Garivani S, Aghakouchak AA. An energy based method for seismic design of frame structures equipped with metallic yielding dampers considering uniform inter-story drift concept. Eng Struct 2020;205:11:114. [CrossRef]
[14] Liu Y, Wu J, Donà M. Effectiveness of fluid-viscous dampers for improved seismic performance of inter-storey isolated buildings. Eng Struct 2018;169:276–292. [CrossRef]
[15] Naeim F, Kelly JM. Design of seismic isolated structures: from theory to practice. New York: John Wiley & Sons; 1999. [CrossRef]
[16] Tonyali Z, Yurdakul M, Sesli H. Dynamic Response of Concentrically Braced Steel Frames to Pulse Period in Near-Fault Ground Motions. Turk J Sci Technol 2022;17:357–373. [CrossRef]
[17] Scawthorn C, Chen W-F. Earthquake engineering handbook. Boca Raton, Philadelphia: CRC Press; 2002. [CrossRef]
[18] Bhuiyan AR, Okui Y, Mitamura H, Imai T. A rheology model of high damping rubber bearings for seismic analysis: Identification of nonlinear viscosity. Int J Solids Struct 2009;46:1778–1792. [CrossRef]
[19] Kelly JM. Base isolation: origins and development. EERC News. 1991;12:1–3.
[20] Bhuiyan AR, Alam MS. Seismic performance assessment of highway bridges equipped with superelastic shape memory alloy-based laminated rubber isolation bearing. Eng Struct 2013;49:396–407. [CrossRef]
[21] Yurdakul M, Ateş Ş, Tonyali Z. Comparative Study of Non-Isolated and Isolated Bridge with TCFP Bearing Under Spatially Varying Ground Motions. Int J Comput Exp Sci Eng 2017;3:29–32.
[22] Kiral A, Ergün M, Tonyali Z, Artar M, Şentürk I. A case study comparing seismic retrofitting techniques for a historically significant masonry building's minaret. Eng Fail Anal 2024;166:1–40. [CrossRef]
[23] Chang C-H. Modeling of laminated rubber bearings using an analytical stiffness matrix. Int J Solids Struct 2002;39:6055–6078. [CrossRef]
[24] Seo J, Hu JW. Seismic response and performance evaluation of self-centering LRB isolators installed on the CBF building under NF ground motions. Sustainability 2016;8:109. [CrossRef]
[25] Haque MN, Zisan MB, Bhuiyan AR. Seismic response analysis of base isolated building: Effect of lead rubber bearing characteristics. Malaysian J Civ Eng 2013;25:154–167. [CrossRef]
[26] Santhosh HP, Manjunath KS, Kumar KS. Seismic analysis of low to medium rise building for base isolation. Int J Res Eng Technol 2013;2:1–5. [CrossRef]
[27] Fakih M, Hallal J, Darwich H, Damerji H. Effect of Lead-Rubber Bearing Isolators in Reducing Seismic Damage for a High-Rise Building in Comparison with Normal Shear Wall System. Struct Durabil & Health Monitor 2021;15:247. [CrossRef]
[28] Ren X, Lu W, Zhu Y, He Y, Li T. Compressive behavior of low shape factor lead-rubber bearings: Full-scale testing and numerical modeling. Eng Struct 2020;209:110030. [CrossRef]
[29] Sesli H, Tonyali Z, Yurdakul M. An investigation on seismically isolated buildings in near-fault region. J Innov Eng Nat Sci 2022;2:47–65. [CrossRef]
[30] Bhandari M, Bharti SD, Shrimali MK, Datta TK. Applicability of capacity spectrum method for base-isolated building frames at different performance points. J Earthq Eng 2021;25:270–299. [CrossRef]
[31] Chanda A, Debbarma R. Probabilistic seismic analysis of base isolated buildings considering near and far field earthquake ground motions. Struct Infrastruct Eng 2021;18:97–108. [CrossRef]
[32] Mousazadeh M, Pourreza F, Basim MC, Chenaghlou MR. An efficient approach for LCC-based optimum design of lead-rubber base isolation system via FFD and analysis of variance (ANOVA). Bullet Earthq Eng 2020;18:1805–1827. [CrossRef]
[33] Ye K, Xiao Y, Hu L. A direct displacement-based design procedure for base-isolated building structures with lead rubber bearings (LRBs). Eng Struct 2019;197:109402. [CrossRef]

[34] Choun Y-S, Park J, Choi I-K. Effects of mechanical property variability in lead rubber bearings on the response of seismic isolation system for different ground motions. Nucl Eng Technol 2014;46:605–618. [CrossRef]
[35] Kanbir Z, Alhan C, Özdemir G. Influence of superstructure modeling approach on the response prediction of buildings with LRBs considering heating effects. Structures 2020;28:1756–1773. [CrossRef]
[36] Wang SJ, Lin WC, Chiang YS, Hwang JS. Mechanical behavior of lead rubber bearings under and after nonproportional plane loading. Earthq Eng Struct Dyn 2019;48:1508–1531. [CrossRef]
[37] Shi Y, Saburi K, Nakashima M. Second-mode tuned mass dampers in base-isolated structures for reduction of floor acceleration. Earthq Eng Struct Dyn 2018;47:2519–2538. [CrossRef]
[38] Deringöl AH, Güneyisi EM, Hansu O. Combined Effect of Bearing Stiffness of the Base Isolator and Damping Characteristics of the Viscous Damper on the Nonlinear Response of Buildings. Int J Steel Struct 2022;22:1497–1517. [CrossRef]
[39] Oesterle MG. Use of incremental dynamic analysis to assess the performance of steel moment-resisting frames with fluid viscous dampers. Virgina, USA: Virginia Tech; 2003.
[40] Castaldo P, Castaldo P. Passive energy dissipation devices. Integrated Seismic Design of Structure and Control Systems. 2014:21–62. [CrossRef]
[41] Politopoulos I. A review of adverse effects of damping in seismic isolation. Earthq Eng Struct Dyn 2008;37:447–465. [CrossRef]
[42] Boksmati JI, Madabhushi GS, Thusyanthan IN. Dynamic soil-structure interaction of a shallow founded shear frame and a frame equipped with viscous dampers under seismic loading. Eng Struct 2021;227:111388. [CrossRef]
[43] Chang K-C, Lin Y-Y, Chen C-Y. Shaking table study on displacement-based design for seismic retrofit of existing buildings using nonlinear viscous dampers. J Struct Eng 2008;134:671–681. [CrossRef]
[44] Hwang JS, Hung CF, Huang YN, Wang SJ. Design force transmitted by isolation system composed of lead-rubber bearings and viscous dampers. Int J Struct Stabil Dyn 2010;10:287–298. [CrossRef]
[45] Ganji M, Kazem H. Comparing seismic performance of steel structures equipped with viscous dampers and lead rubber bearing base isolation under near-field earthquake. Civ Eng J 2017;3:124–136. [CrossRef]
[46] Domenico DD, Ricciardi G, Takewaki I. Design strategies of viscous dampers for seismic protection of building structures: a review. Soil Dyn Earthq Eng 2019;118:144–165. [CrossRef]
[47] Zhou Y, Xing L. Seismic performance evaluation of a viscous damper-outrigger system based on response spectrum analysis. Soil Dyn Earthq Eng 2021;142:106553. [CrossRef]
[48] Kiral A, Tonyali Z. Seismic Response Control of Buildings Using Viscous-Based Devices, Modern Approaches to Traffic Safety and Sound Insulation, Chapter 4, BIDGE Publications, pp. 70-111, 2024.
[49] Kiral A, Garcia R, Petkovski M, Hajirasouliha I. Seismic performance assessment of steel buildings equipped with a new semi-active displacement-dependent viscous damper. J Earthq Tsunami 2024;18. [CrossRef]
[50] Kiral A, Gurbuz A, Ustabas I. The Seismic Response Evaluation of an Existing Multi-span Reinforced Concrete Highway Bridge in the Presence of Linear and Nonlinear Viscous Dampers. Arab J Sci Eng 2024:1–19. [CrossRef]
[51] Domenico DD, Ricciardi G. Earthquake-resilient design of base isolated buildings with TMD at basement: Application to a case study. Soil Dyn Earthq Eng 2018;113:503–521. [CrossRef]
[52] Yaktine AER, Titirla M, Larbi W. Effects of LRB Isolators and Viscous Dampers on Seismic Isolated Irregular Reinforced Concrete Buildings. In International Conference on Acoustics and Vibration Cham: Springer International Publishing; 2022. p. 116–124. [CrossRef]
[53] Hatipoglu YS, Duzgun OA. Investigation of the effectiveness of viscous dampers connected to adjacent buildings on dynamic behavior under soil-structure interaction effects. Sigma J Eng Nat Sci 2020;11:51–72.
[54] Thakur R, Tiwary AK. Comparative study on the effectiveness of fluid viscous dampers and base isolation: an approach toward enhancing seismic performance of composite structures. Innov Infrastruct Solut 2023;8:267. [CrossRef]
[55] Dan M, Kohiyama M. System identification and control improvement of a semi-active-controlled base-isolated building using the records of the 2011 Great East Japan earthquake. In 11th International Conference on Structural Safety and Reliability, ICOSSAR 2013 2013. p. 3841–3847. [CrossRef]
[56] MATLAB-R. Available at: https://it.mathworks.com/help/matlab/ Accessed Feb 12, 2024.
[57] Kohiyama M, Omura M, Takahashi M, Yoshida O, Nakatsuka K. Update of control parameters for semi-actively controlled base-isolated building to improve seismic performance. Japan Architect Rev 2019;2:226–237. [CrossRef]
[58] Yoshida K. First building with semi-active base isolation. J Jpn Soc Mech Eng 2001;104:698.
[59] NOAA. National Centers for Environmental Information Available at: https://ngdc.noaa.gov/hazard/dart/2011honshu_dart.html Accessed Feb 12, 2024.